Supplementary Information

Supplemental methods

*siRNA transfection***.** miRNA inhibitors (Ambion) are single-stranded, chemically modified oligonucleotides designed to inhibit endogenous miRNAs. For in vitro miRNA inhibition studies, cells were transfected with anti-miR-545 and anti-miR-630 (200 nmol/L) using Lipofectamine 2000 (Invitrogen) according to the manufacturer's instructions. Forty-eight hours after transfection, cells were used for migration and invasion assays, luciferase reporter assays, and Western blot assays.

Cell tracing using a time-lapse microscope imaging system. Cells were seeded onto 6 cm dishes and grown in culture medium supplemented with 10% FBS. After 8 hours, cells placed into a fluorescence microscope (Axioplan 2, Zeiss) equipped with a charge-couple device camera (Axiocam, Zeiss) and incubated at 37 °C in humidified 5% CO_2. Cells were imaged every 15 minutes over a 24 hours period and were quantified using the image J system (U.S. National Institutes of Health, Bethesda, MD, USA).

*MTT proliferation assay***.** The assay provided in a cell proliferation kit (MTT, Roche) was performed in 96-well plates according to the manufacturer's instructions.

Lentiviral infections. The lentiviral ANGPTL1, Slug, integrin α_1, integrin α_2, integrin β_1, Sp-1 and C/EBPα shRNA constructs were purchased from the National

RNAi Core Facility, Taiwan. Lentiviruses were produced by co-transfecting the shRNA-expressing vector, pMD.G and pCMVΔ8.91 constructs into 293T cells using calcium phosphate. Viral supernatants were harvested, filtered with a 0.45 μm filter, and used to infect cells with 8 μg/mL polybrene. Cells were selected using 2 μg/mL puromycin.

Migration and invasion assays. Migration and invasion assays were performed by using trans-well inserts for a 24-well plate containing 8 μm pores (Millipore). Filters coated with Matrigel (70 μg, BD) were used for the invasion assay. In both assays, cells were plated in culture medium without serum or growth factors in the upper chamber, and medium supplemented with serum was used as a chemoattractant in the lower chamber. Cells ($2x10^4$ cells for migration assay and $1x10^5$ for invasion assay) were incubated for 24 hours and cells that did not migrate or invade through the pores were removed by a cotton swab. Cells on the lower surface of the membrane were fixed with methanol, stained with crystal violet, and counted under the microscope. The numbers of cells that migrated and invaded were normalized to the growth rate by MTT assay for each cell line.

Wound-healing migration assay. For wound-healing migration assays, cells were seeded on 6-well plates at a density of 80% in culture medium, and incubated for 24 hours. The confluent monolayer was then scratched with a fine pipette tip, and

migration was visualized by microscopy. The rate of wound closure was determined from observations made at the indicated times.

RNA isolation, reverse transcription PCR, and real-time PCR. Total RNA was isolated using Trizol (Invitrogen) according to the manufacturer's instructions, and 2 μg were reverse-transcribed into single-stranded cDNA using Moloney murine leukemia virus (M-MLV) reverse transcriptase buffer (Invitrogen) containing 10 mM dithiothreitol, all four deoxynucleoside 5'-triphosphate (dNTP; each at 2.5 mM), 1μg of (dT) 12-18 primer, and 200 U of M-MLV reverse transcriptase. The reaction mixture was incubated at 42 °C for 1.5 hours, and the reaction was terminated by heating at 99 °C for 5 minutes. PCR was used to amplify 1 μl of cDNA using specific pairs of primers (primers sequences are shown in Supplementary Table S1). PCR amplifications were carried out in reaction buffer containing 20 mM Tris–HCl (pH 8.4), 50 mM KCl, 1.5 mM $MgCl_2$, all four dNTPs (each at 6.25 μM), 2.5U of Taq DNA polymerase, and 0.5 μM of each primer. The reactions were performed in a Biometra Thermoblock (Biometra). PCR products were analysed using agarose gel electrophoresis. For real-time PCR, miRNA-specific TaqMan RT primers (Applied Biosystems) were used to perform reverse transcription. Real-time PCR was performed using an Applied Biosystems 7900 Fast Real Time PCR system with miRNA-specific primers and gene-specific primers (Applied Biosystems)

(Supplementary Table S1) and TaqMan Universal PCR Master Mix (Applied Biosystems). Values represent the average of three independent experiments, normalized to the *β-actin* or RNU-6B. For pre-miR-630 detection, the RT primers were designed according to the report by Varkonyi-Gasic and Hellens (1). The sequences of precursor miRNAs obtained from the miRbase website (http://www.mirbase.org/index.shtml) were as follows: miR-630 RT primer, 5'-ATATAGTTAAGAACTACCTTCCCTGG-3'. The reactions were incubated at 37°C for 50 minutes, reactions were terminated by incubating at 85°C for 15 minutes to inactivate the reverse transcriptase. Transcripts were detected by quantitative PCR with the LightCycler FastStart DNA Master SYBR Green I kit (Roche) with the LightCycler 480 (Roche). PCR reactions contained 0.5 μ mol/L of each forward and reverse primer, 1×Master SYBR Green Master mix, and 2 μ L of cDNA. Amplification curves were generated with an initial denaturing step at 95°C for 10 minutes, followed by 50 cycles of 95°C for 10 seconds, 60°C for 5 seconds, and 72°C for 7 seconds. The sequences of pre-miR-630 and internal reference β-actin primers are shown in Supplementary Table S1.

Enzyme-Linked Immunosorbent Assay (*ELISA).* Integrin $\alpha_1\beta_1$ recombinant protein in PBS was immobilized onto 96-well polystyrene ELISA plates and incubated overnight at 4°C. Plates were then blocked with 0.5% BSA and washed

following standard ELISA techniques. ANGPTL1 recombinant protein, collagen, BSA or ANGPTL1 recombinant protein with indicated antibodies was incubated 12 hours (or overnight) at 4°C. After this incubation, the plates were washed thrice with PBS and the amount of ANGPTL1 or collagen bound to the immobilized plate was determined with specific primary antibodies for ANGPTL1 or collagen 2 hours at room temperature. After incubation with the respective horseradish peroxidase conjugate secondary antibodies for 1 hour at 37°C, the TMB solution (Sigma-Aldrich) was added for 30 minutes, and the reaction was stopped by the addition equal volume of stopping solution. The absorbance was recorded at 450 nm.

Specimens and immunohistochemistry. The tissues used were from the Cancer Tissue Core of the National Taiwan University Hospital. The surgical specimens had been fixed in formalin and embedded in paraffin before they were archived. We used the archived specimens for immunohistochemical staining. The tissue sections were deparaffinized, soaked in 10 μM sodium citrate and boiled in the autoclave for 15 minutes to retrieve cell antigens. The primary antibodies were applied to the slides and incubated at 4°C overnight. The slides were washed and then the slides were stained by the Super Sensitive Link-Label IHC Detection System (Biogenex Laboratories), counterstained with hematoxylin, dehydrated and mounted. A four-point staining intensity scoring system was devised for determining the relative

expression of ANGPTL1 and Slug in cancer specimens; the staining intensity score ranged from 0 (no expression) to 3 (maximal expression). The results were classified into two groups according to the intensity and extent of staining: in the low-expression group, staining was observed in 0–1% of the cells (staining intensity score = 0), or in less than 10% of the cells (staining intensity score =1); in the high-expression group, staining was present in 10%–50% of the cells (staining intensity score = 2), or more than 50% of the cells (staining intensity score = 3). All of the immunohistochemical staining results were reviewed and scored independently by two pathologists. For miR-630 detection, microRNA was isolated from paraffinised tissue using the High Pure FFPE RNA Micro Kit (Roche) and real-time PCR was performed as described previously. The results were classified into two groups according to relative miR-630 expression levels (ΔCt). The relative level of miR-630 expression in the low-expression group was ΔCt > averageΔCt, while the relative level of miR-630 expression in the high-expression group was ΔCt < averageΔCt. For quantification of ANGPTL1 expression, images were acquired using Tissuequest software (Tissue Gnostics). The percentage of cells positive for ANGPTL1 expression was determined using Histoquest software (Tissue Gnostics).

Luciferase reporter assay. The 3'UTR of human *SNAI2* was amplified using PCR and cloned into a pMIR-Report vector. The segment of the *SNAI2* 3′UTR

containing the mutant miR-545 and miR-630 target sequences were also cloned into the pMIR-REPORT Luciferase vector (Ambion) using a QuickChange II Site-Directed Mutagenesis Kit (Stratagene). The promoter construct of human miR-630 (~1.5 kb) and a series of promoter fragments were amplified using PCR and cloned into a pGL3-basic vector. Cells (50% confluent in 24-well plates) were transfected with indicated plasmids by Lipofectamine 2000 (Invitrogen). A firefly luciferase reporter gene construct and the pTK-Renilla luciferase construct (for normalization) were co-transfected at 1 μg each per well. Cell extracts were harvested 48 hours after transfection, and luciferase activity was measured using the Dual-Luciferase Reporter Assay System (Promega). The segment of the miR-630 promoter containing the mutant Sp-1 site was cloned into the pGL3-basic vector using a QuickChange II Site-Directed Mutagenesis Kit (Stratagene). The mutation primers of Sp1 binding sequence are forward: 5'-GCAGTGACGCAAAGATTAGTGACGC GACGACGC-3'and reverse: 5'-GCGTCGTCGCGTCACTAATCTTTGCGTCACTG C-3'

ChIP assay. Chromatin immunoprecipitation (ChIP) assays were performed according to the manufacturer's protocol (Upstate Biotechnology). Cells were harvested after cross-linking with 1% formaldehyde. The nuclei were released with SDS Lysis Buffer and sonicated with a MISONIX Sonicator 3000 (Misonix). The

soluble chromatin at 200 ml per immunoprecipitation assay were diluted 10-fold in ChIP Dilution Buffer and then the lysate was precleared with Protein A Agarose/Salmon Sperm DNA (50% Slurry) for 30 minutes at 4 °C. The precleared lysate and the mixtures were incubated with specific antibodies (Supplementary Table S2) and rotated at 4°C overnight. The immunocomplexes were pulled down by Protein A Agarose/Salmon Sperm DNA (50% Slurry) and then washed with the Low-Salt Immune Complex Wash Buffer, the High-Salt Immune Complex Wash Buffer, the LiCl Immune Complex Wash Buffer and finally two times with TE Buffer. The bound protein was eluted with elution buffer containing 1% SDS and 0.1M $NaHCO_3$. The crosslinks were reversed by heating at 65°C for 4 hours. The DNA was purified by the QIAquick PCR purification Kit (QIAGEN) and analyzed by quantitative PCR using specific primers as described in Supplementary Table S1.

ECM cell adhesion assay. The colorimetric ECM Cell Adhesion Array kit (Chemicon) with ECM protein-coated 96-well plates was used for adhesion assays. Cells were harvested, resuspended in Assay Buffer, seeded onto plates, and incubated at 37 °C for 1 hour. After incubation, the medium was gently removed from the wells to remove nonattached cells. Each well was washed with Assay Buffer. Attached cells were stained with Cell Stain Solution and eluted using Extraction Buffer for 10 minutes. Cell adhesion was quantified by measuring the absorbance of the eluted

buffer at 540–570 nm with a microplate reader.

Analysis of secreted protein expression. For analysis of secreted protein expression, cells were seeded onto 6-well plates at a density of 90% in serum free medium, and conditional medium was collected 48 hours later. Medium was cleared of cells by centrifuging at 2500*g* for 5 minutes. ANGPTL1 concentrations were detected in conditional medium using an ELISA kit (Uscn Life Science Inc.).

1. Varkonyi-Gasic, E., and Hellens, R.P. Quantitative stem-loop RT-PCR for detection of microRNAs. *Methods Mol Biol.* 2011;744:145-157.

Supplemental Figure Legends

Supplementary Figure 1. ANGPTL1 has higher expression in primary lung tumors than in lymph node metastatic tumors. (**A**) Specificity of ANGPTL1 antibody for immunohistochemistry. ANGPTL1 staining was less detectable in blocking antigen addition groups. Scale bars, 100 μm. (**B**) Representative images of normal parts, lung primary tumors and matched lymph node metastatic tumors from the same patient. Scale bars, 100 μm. (**C**) The percentage of ANGPTL1-positive cells was quantified by Histoquest software in normal parts, lung primary tumors and matched lymph node metastatic tumors from the same patient. (**D**) The average percentage of ANGPTL1 positive cells. Data are shown as mean ± SE. **P*<0.05, ***P*<0.01. (two-tailed Student's t-test).

Supplementary Figure 2. ANGPTL1 inversely correlates with lymph node metastasis in other cancers. (A) Staining with the normal mouse IgG as negative control. Scale bars, 100 μm. (B) Strong staining of ANGPTL1 in normal parts. Scale bars, 100 μm. (C) Strong staining of ANGPTL1 (high expression). Scale bars, 100 μm. (D) Weak staining of ANGPTL1 (low expression). Scale bars, 100 μm. (E) Percentage of patients with high expression of ANGPTL1 and low expression of ANGPTL1 in different lymph nodes status. **P*<0.05. (n=52, two-sided Pearson chi-square test). (F)

The expression levels of *ANGPTL1* mRNA in primary prostate tumors (n=66) and lymph node metastatic tumors (n=15) from a public dataset (GSE6919). *P<0.05. (two-tailed Student's t-test).

Supplementary Figure 3. ANGPTL1 inhibits lung and breast cancer cell migration and invasion. (**A**) The relative migration and invasion in lung and breast cancer cells. (**B**) The *ANGPTL1* expression and secreted ANGPTL1 level in lung and breast cancer cells. (**C**) Effects of ANGPTL1 overexpression and knockdown on cell proliferation. MTT assay showing cell proliferation in CL1-5 cells (top) expressing pcDNA3.1 and ANGPTL1 for various periods of time and H928 cells (bottom) expressing shRNA-Luc, shRNA-ANGPTL1-1 and shRNA-ANGPTL1-2 for various periods of time. (**D**) Measurement of the relative migration in ANGPTL1 overexpression CL1-5 and ANGPTL1 knockdown H928 cells. Top, representative images of wound healing migration assay. Bottom, quantification of wound healing migration assay. (**E**) Western blot analysis of ANGPTL1 in conditional medium (CM) (top). Treatment of CL1-5 cells with conditional medium from 293T/ANGPTL1 and measurement of the relative migration and invasion of cancer cells (bottom). The antibody-bound ANGPTL1 in conditioned medium were removed prior migration and invasion assays. (**F**) Treatment with 50 ng/ml rANGPTL1, 50 ng/ml rGST and vehicle (PBS) in CL1-5,

A549 and MDA-MB-231/I3 cells and measurements of the relative migration and invasion of cancer cells. (G) Weights of lungs in individual mice (tail vein injection). (H) RT-PCR analysis of *ANGPTL1* from lungs of individual mice. Data are shown as mean ± SE. **P*<0.05, ***P*<0.01. (two-tailed Student's t-test).

Supplementary Figure 4. ANGPTL1 represses epithelial-to-mesenchymal transition by targeting Slug in lung and breast cancers. (**A**) Phase-contrast images of ANGPTL1 overexpression MDA-MB-231/I3 cells (top) and ANGPTL1 knockdown MDA-MB-231 cells (bottom). Scale bars, 100 μm. (**B**) Western blot analysis of E-cadherin, N-cadherin, fibronectin and vimentin in ANGPTL1 overexpression MDA-MB-231/I3 cells (left) and ANGPTL1 knockdown MDA-MB-231 cells (right). (**C**) Western blot analysis of Slug, Snail, Foxc2 and Twist in ANGPTL1 overexpression MDA-MB-231/I3 cells (left) and ANGPTL1 knockdown MDA-MB-231 cells (right). (**D**) Weights of the left lungs in individual mice (lung orthotopic injection). (**E**) Weights of lungs in individual mice (tail vein injection). Data are shown as mean ± SE. **P*<0.05, ***P*<0.01. (two-tailed Student's t-test).

Supplementary Figure 5. Knockdown of Slug inhibits shANGPTL1-induced lung cancer cell motility and metastasis. (**A**) RT-PCR analysis of *ANGPTL1* and Western

blot analysis of Slug in ANGPTL1 knockdown CL1-0GL cells infected with shRNA-LacZ and shRNA-Slug. (**B**) Measurement of the migration and invasion in ANGPTL1 knockdown CL1-0GL cells infected with shRNA-LacZ and shRNA-Slug. (**C**) Representative luciferase images of mice. Top, lung orthotopic injection. Bottom, tail vein injection. (**D**) Lungs were isolated and examined after lung orthotopic injection (top) and tail vein injection (bottom). Upper panel: Histological analyses of lung metastatic tumors by haematoxylin and eosin staining. Scale bars, 500 μm. Lower panel: representative luciferase activity images. Scale bars, 5 mm. (**E**) The numbers of lung metastatic nodules. Top, lung orthotopic injection. Bottom, tail vein injection. (**F**) Weights of the left lungs in individual mice (lung orthotopic injection). (**G**) Weights of lungs in individual mice (tail vein injection). Data are shown as mean ± SE. **P*<0.05, ***P*<0.01. (two-tailed Student's t-test).

Supplementary Figure 6. ANGPTL1 represses Slug protein expression, not RNA expression. (**A**) Western blot analysis of Slug, Snail, Foxc2, and Twist in ANGPTL1 overexpression A549 cells (left) and ANGPTL1 knockdown H928 cells (right). (**B**) qRT-PCR analysis of *Slug* expression in ANGPTL1 overexpression CL1-5, A549 and MDA-MB-231/I3 cells (top) and ANGPTL1 knockdown CL1-0, MDA-MB-231 and H928 cells (bottom). (**C**) Western blot analysis of Slug and Snail in CL1-5 cells

treated with 50 ng/ml rANGPTL1 for various periods of time. (**D**) qRT-PCR analysis of *Slug* expression in CL1-5 cells treated with 50 ng/ml rANGPTL1 for various periods of time. (**E**) Immunohistochemical staining of ANGPTL1 and Slug in samples from lung cancer patients. Scale bars, 100 μm. (**F**) Percentage of lung cancer patients expressing high and low levels of ANGPTL1 among those expressing high and low levels of Slug. $^{**}P<0.01$. (n=102, two-sided Pearson chi-square test).

Supplementary Figure 7. ANGPTL1 represses Slug-protein expression through post-transcriptional regulation. (**A**) Western blot analysis (top) of Slug in ANGPTL1 overexpression MDA-MB-231/I3 cells after treatment with 10 μM MG132. Quantification of Slug expression from Western blots following normalization to α-tubulin levels. Slug levels were arbitrarily assigned a value of 1 in MDA-MB-231/I3/pcDNA3.1 cells. (**B**) Western blot analysis (top) of Slug in ANGPTL1 overexpression MDA-MB-231/I3 cells after treatment with 10 μg/ml cycloheximide (CHX). Quantification of Slug from Western blot following normalization to α–tubulin levels (bottom). Slug levels from MDA-MB-231/I3/pcDNA3.1 and MDA-MB-231/I3/ANGPTL1 were arbitrarily assigned a value of 100% at 0 hour. (**C-D**) qRT-PCR analysis of miR-545 and miR-630 expression in ANGPTL1 overexpression CL1-5 cells transiently transfected

with anti-miR-545 (**C**) and anti-miR-630 (**D**). (**E**) qRT-PCR analysis of *Slug* expression in ANGPTL1 overexpression CL1-5 transiently transfected with anti-miR-630. Data are shown as mean ± SE. **P*<0.05, ***P*<0.01. (two-tailed Student's t-test).

Supplementary Figure 8. ANGPTL1/Slug expression levels correlate with miR-630 expression levels, and miR-630 expression inversely correlates with stage, lymph node status, invasion, and poor prognosis of lung cancer. (**A**) qRT-PCR analysis of relative miR-630 expression (ΔCt) in lung cancer patients, stratified by average ΔCt. Percentage of patients with high and low expression of ANGPTL1 in those expressing high and low levels of miR-630. (**B**) qRT-PCR analysis of relative miR-630 expression (ΔCt) in lung cancer patients, stratified by average ΔCt. Percentage of patients with high expression of Slug and low expression of Slug in lung cancer patients expressing high miR-630 and low miR-630. (**C-E**) Percentage of patients with high and low expression of miR-630 according to different clinical parameters as follows: D. stage, E. lymph node status, F. cancer type (AC: invasive adenocarcinoma; BAC: Bronchoalveolar carcinoma). **P*<0.05, ***P*<0.01. (A-D, n=73, E, n=46, two-sided Pearson chi-square test). (**F**-**G**) Kaplan-Meier plot of overall (**F**) and disease-free (**G**) survival of lung cancer patients, stratified by miR-630 expression.

The log rank test was used to compare differences between groups (n=73).

Supplementary Figure 9. ANGPTL1 induces pri-miR-630 and pre-miR-630 expression. (A-B) qPT-PCR analysis of pri- and pre-miR-630 in ANGPTL1 overexpression CL1-5 cells (A) and ANGPTL1 knockdown CL1-0 cells (B). Data are shown as mean ± SE. *P<0.05. (two-tailed Student's t-test).

Supplementary Figure 10. Cell adhesion ability in CL1-5/pcDNA3.1 and CL1-5/ANGPTL1 cells. ECM cell adhesion array analysis of adhesion ability in ANGPTL1 overexpression CL1-5 cells. Data are shown as mean ± SE. *P<0.05, **P<0.01. (two-tailed Student's t-test).

Supplementary Figure 11. Fibrinogen-like domain is required for the binding of ANGPTL1 with integrin $\alpha_1\beta_1$. (**A**) Schematic representation the domain of ANGPTL1 and the different truncated constructs. (**B**) CL1-5 cells were treated with ANGPTL1-CCD and ANGPTL1-FD conditional medium for 2 hours. Cell lysates were immunoprecipitated with anti-V5 and normal IgG. Western blot analysis of V5, integrin α_1, -α_2-, α_6- and -β_1 in this immunoprecipitation.

Supplementary Figure 12. ANGPTL1 inversely correlates with the level of p-ERK in lung cancer patients. (**A**) Western blot analysis of phosphorylation of ERK in lung cancer patients (n=27). Quantification of p-ERK from Western blots following normalization to ERK levels. (**B**) Correlation analysis of p-ERK/ERK and ANGPTL1 (high and low levels) in lung cancer patients.

Supplementary Figure 13. *Integrin* α_1, -α_2 and -β_1 expression in CL1-5 cells. (A) RT-PCR analysis of *integrin* α_1, α_2 and β_1 expression in ANGPTL1 overexpression CL1-5 cells. (B) RT-PCR analysis of *integrin* α_1,-α_2 and -β_1 expression in CL1-5 cells infected with shRNA-Luc, shRNA-integrin α_1, shRNA-integrin α_2 and shRNA-integrin β_1.

Supplementary Figure 14. C/EBPα is not involved in ANGPTL1-induced miR-630 and repression of Slug. Western blot analysis (top) of C/EBPα, Slug, and qRT-PCR analysis (bottom) of miR-630 expression in ANGPTL1 overexpression CL1-5 cells infected with shRNA-Luc and shRNA-C/EBPα. Data are shown as mean ± SE.

Supplemental Table

Supplementary Table S1

Sequences and information of RT-PCR and qRT-PCR primers.

RT-PCR primers
ANGPTL1
5’-GGGCAAGATGCAAGTACCAT-3’ (forward)
5’-GACACATGGGTGTCTTGTCG-3’ (reverse)
Integrin α1
5’-GAAAATGGGCCTGTTCTTGA-3’ (forward)
5’-TTCAGGAGGTTCTTCGCTGT-3’ (reverse)
Integrin α2
5’-CACTCGATTTGGTTCAGCAA-3’ (forward)
5’-GAACCACTTGTCCAAGGCA-3’ (reverse)
Integrin β1
5’-AATGAAGGGCGTGTTGGTAG-3’ (forward)
5’-CACGTTTGCCCTTGAAACTT-3’ (reverse)
GAPDH
5’-ACCCAGAAGACTGTGGATGG-3’ (forward)
5’-GTCCACCACCCTGTTGCTGT-3’ (reverse)

qRT-PCR primers
pre-miR-630 primer
5’-AACTTA ACATCATGCTACCT-3’ (forward)
5’-ATATAGTTAAGA ACTACCTT-3’ (reverse)
β-actin primer (internal reference for pre-miR-630)
5’- GCTCGTCGTCGACAACGGCTC -3’ (forward)
5’- CAAACATGATCTGGGTCATCTTCTC -3’ (reverse)
qChIP primer
5’-GCGGCAGACACCACCAC-3’ (forward)
5’-GGCCGCTGCTATCGCTACTGAG-3’ (reverse)
ANGPTL1
Part No. Hs00907664_m1 (Applied Biosystems)
Slug
Part No. Hs00950344_m1 (Applied Biosystems)
β-actin (internal reference for *ANGPTL1* and *Slug*)
Part No. Hs99999903_m1 (Applied Biosystems)
miR-1
Part No. 4373161 (Applied Biosystems)

miR-30a-5p
Part No. 4373061 (Applied Biosystems)
miR-200c
Part No. 4373096 (Applied Biosystems)
miR-218
Part No. 4373081 (Applied Biosystems)
miR-411
Part No. 4381013(Applied Biosystems)
miR-432
Part No. 4373280 (Applied Biosystems)
miR-485-3p
Part No. 4378095 (Applied Biosystems)
miR-511
Part No. 4373236 (Applied Biosystems)
miR-545
Part No. 4395378 (Applied Biosystems)
miR-630
Part No. 4380970 (Applied Biosystems)
RUN6B

Part No. 4373381 (Applied Biosystems)
pri-miR-630
Hs03304713_pri (Applied Biosystems)

Supplementary Table S2

All proteins detected by antibodies.

Protein	Antibody, catalog number	Application	Dilution
ANGPTL1	R&D systems, AF2204	Western blot, IP*	1:1000, 1:1000
ANGPTL1	Abnova, H00009068-M03	IHC	1:100
α-tubulin	Sigma, T5168-.2ML	Western blot	1:10000
E-cadherin	Cell Signaling, #4065	Western blot	1:1000
N-cadherin	BD, 610921	Western blot	1:1000
Vimentin	BD, 550513	Western blot	1:1000
Fibronectin	Abcam, ab23750	Western blot	1:1000
Slug	Cell Signaling, #9585	Western blot	1:1000
Slug	Gentex, GTX121924	IHC	1:50
Snail	Cell Signaling, #3895	Western blot	1:1000
Twist	Santa Cruz, sc-134136	Western blot	1:250
Foxc2	Abnova, H00002302-M02	Western blot	1:1000

V5	AbD Serotec, MCA1360	Western blot, IP	1:1000
Integrin α1	Abcam, ab78479	Western blot	1:1000
Integrin α2	Santa Cruz, sc-9089	Western blot	1:1000
Integrin α3	Millipore, MAB1952Z-20	Western blot	1:1000
Integrin α5	Millipore, MAB1956Z-20	Western blot	1:1000
Integrin α6	R&D systems, AF1350	Western blot	1:1000
Integrin αV	Santa Cruz, sc-9969	Western blot	1:1000
Integrin α8	Santa Cruz, sc-25713	Western blot	1:1000
Integrin β1	Santa Cruz, sc-9970	Western blot	1:1000
Integrin β3	Santa Cruz, sc-6626	Western blot	1:1000
Integrin β4	Millipore, MAB2060-20	Western blot	1:1000
Integrin β5	Santa Cruz, sc-14010	Western blot	1:1000
Activated Integrin β1	Millipore, MAB2079Z	Western blot	1:1000
Sp-1	Santa Cruz, sc-17824	Western blot , qChIP	1:1000, 1:100
C/EBPα	Santa Cruz, sc-9314	Western blot, qChIP	1:1000, 1:100
p-FAK	Cell Signaling, #3283	Western blot	1:1000
FAK	Cell Signaling, #3285	Western blot	1:1000
p-ERK	Santa Cruz, sc-81492	Western blot	1:1000
ERK	Santa Cruz, sc-93	Western blot	1:1000

p-AKT	Santa Cruz, sc-33437	Western blot	1:1000
AKT	Santa Cruz, sc-8312	Western blot	1:1000
p-p38	Cell Signaling, #9216	Western blot	1:1000
p38	Cell Signaling, #9212	Western blot	1:1000
p-LNK	Santa Cruz, sc-81502	Western blot	1:1000
JNK	Santa Cruz, sc-571	Western blot	1:1000

Abbreviations:

IP: immunoprecipitation (* capture the ANGPTL1 form conditional medium)

IHC: immunohistochemistry

qChIP: quantitative chromatin immunoprecipitation

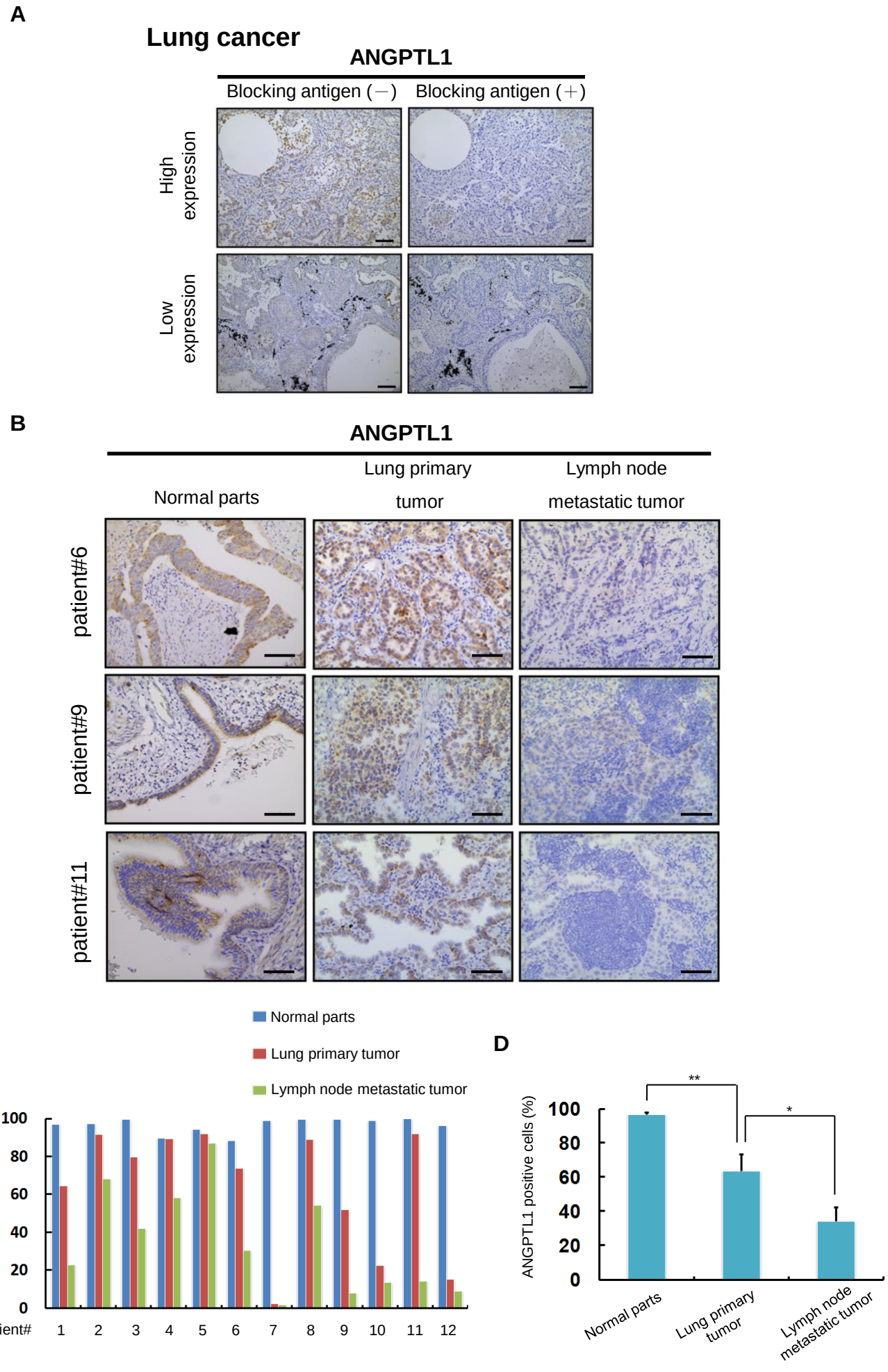

Supplementary Figure 1

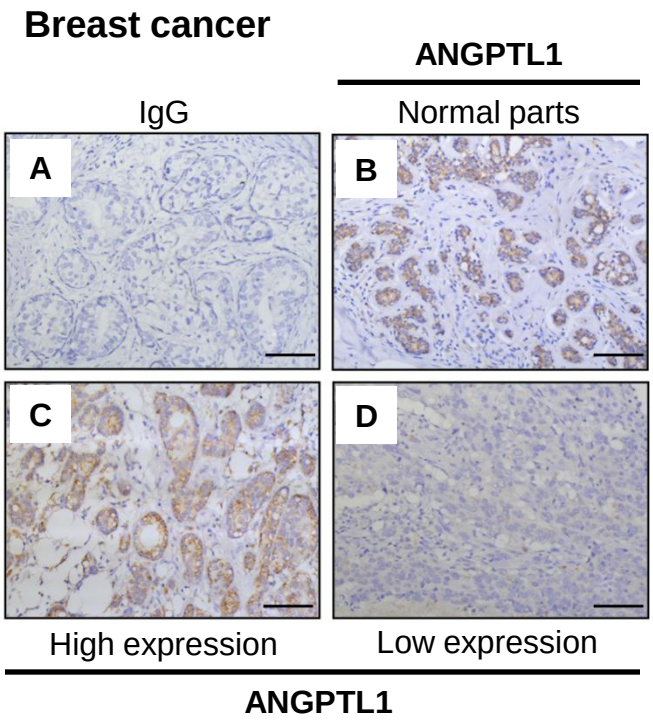

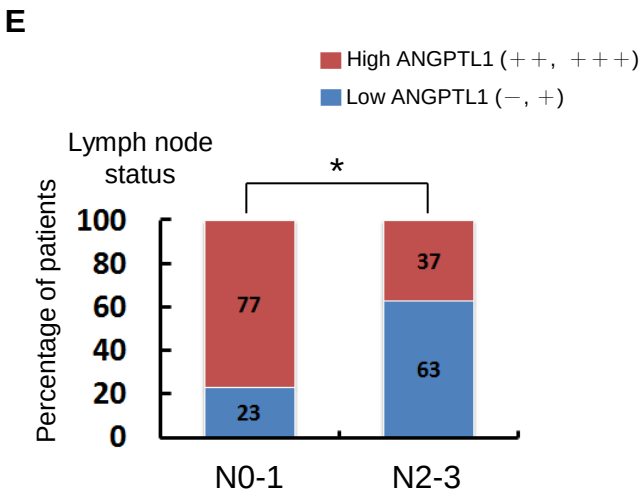

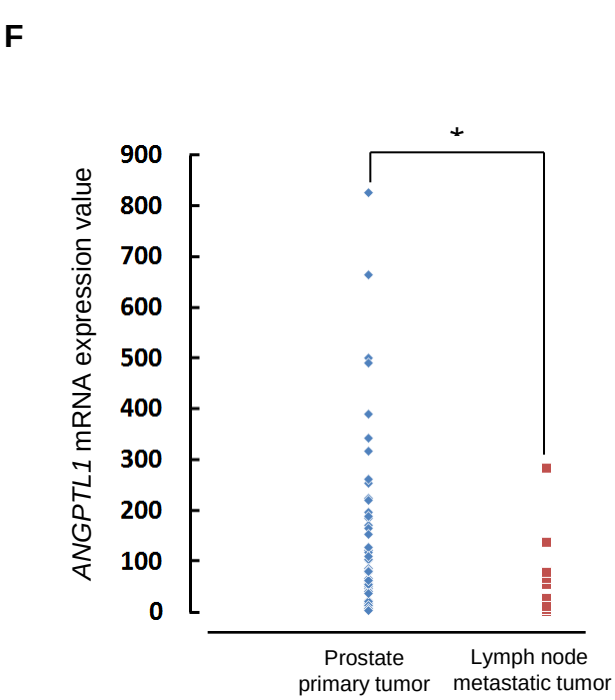

Supplementary Figure 2

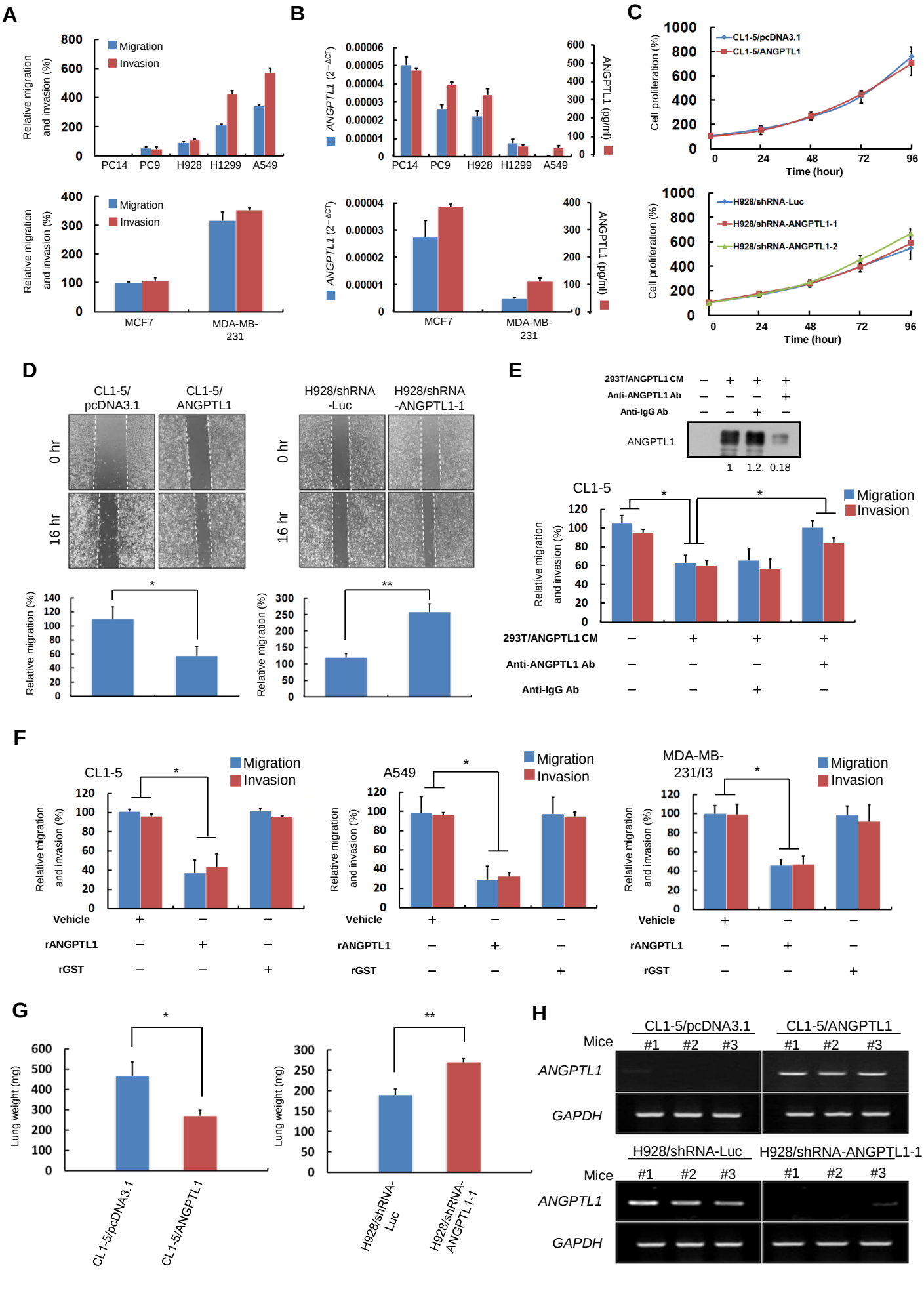

Supplementary Figure 3

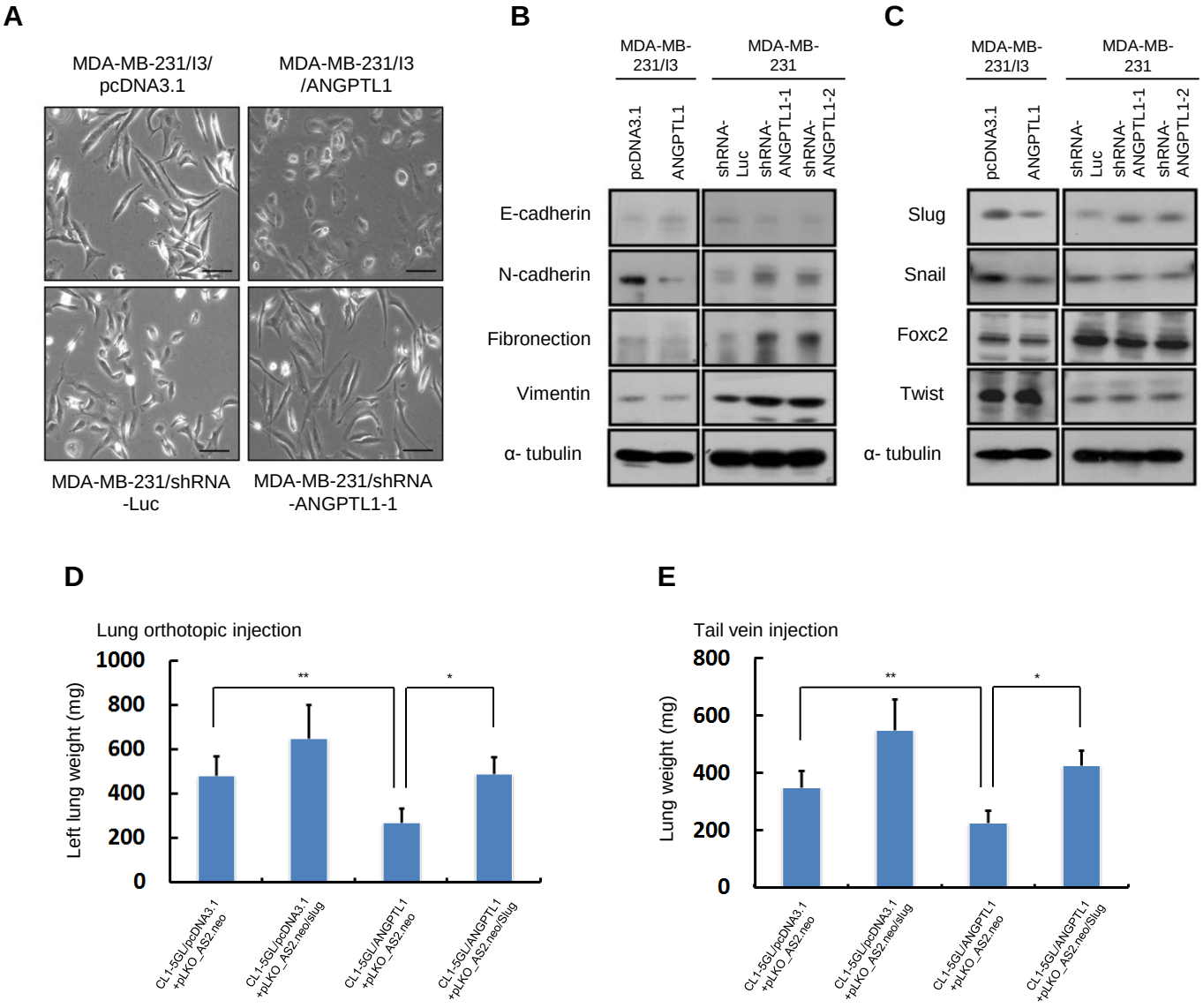

Supplementary Figure 4

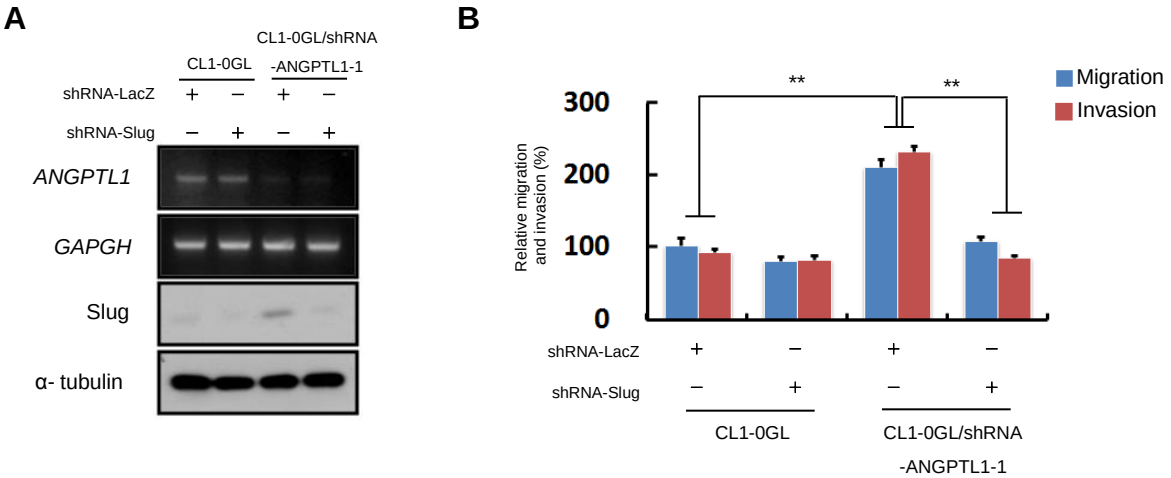

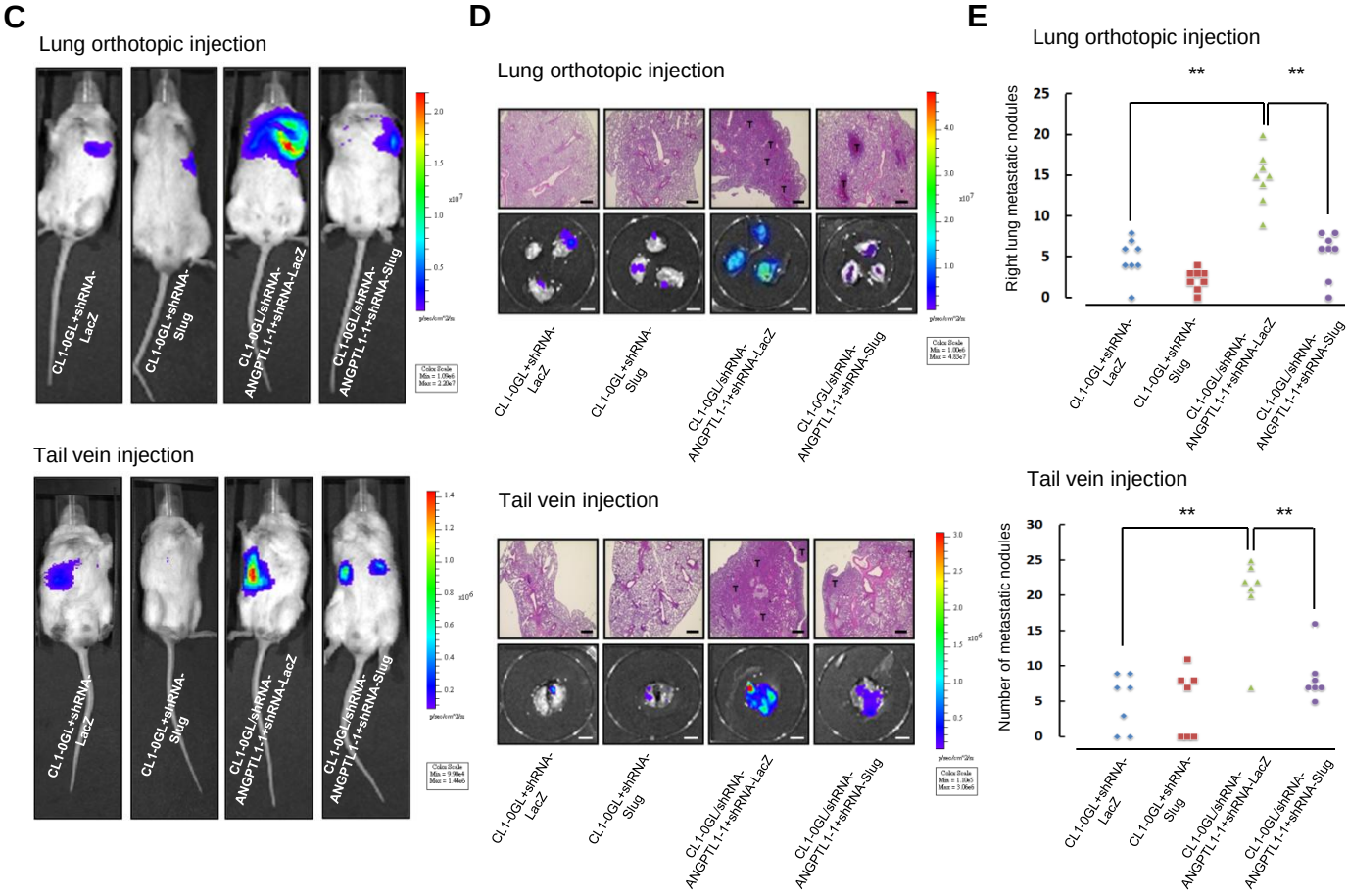

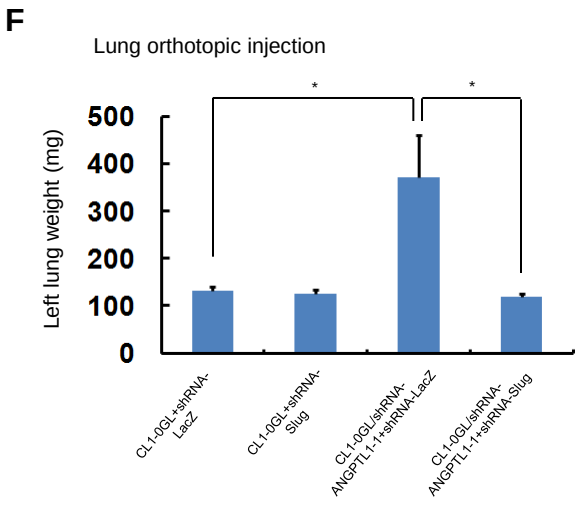

Supplementary Figure 5

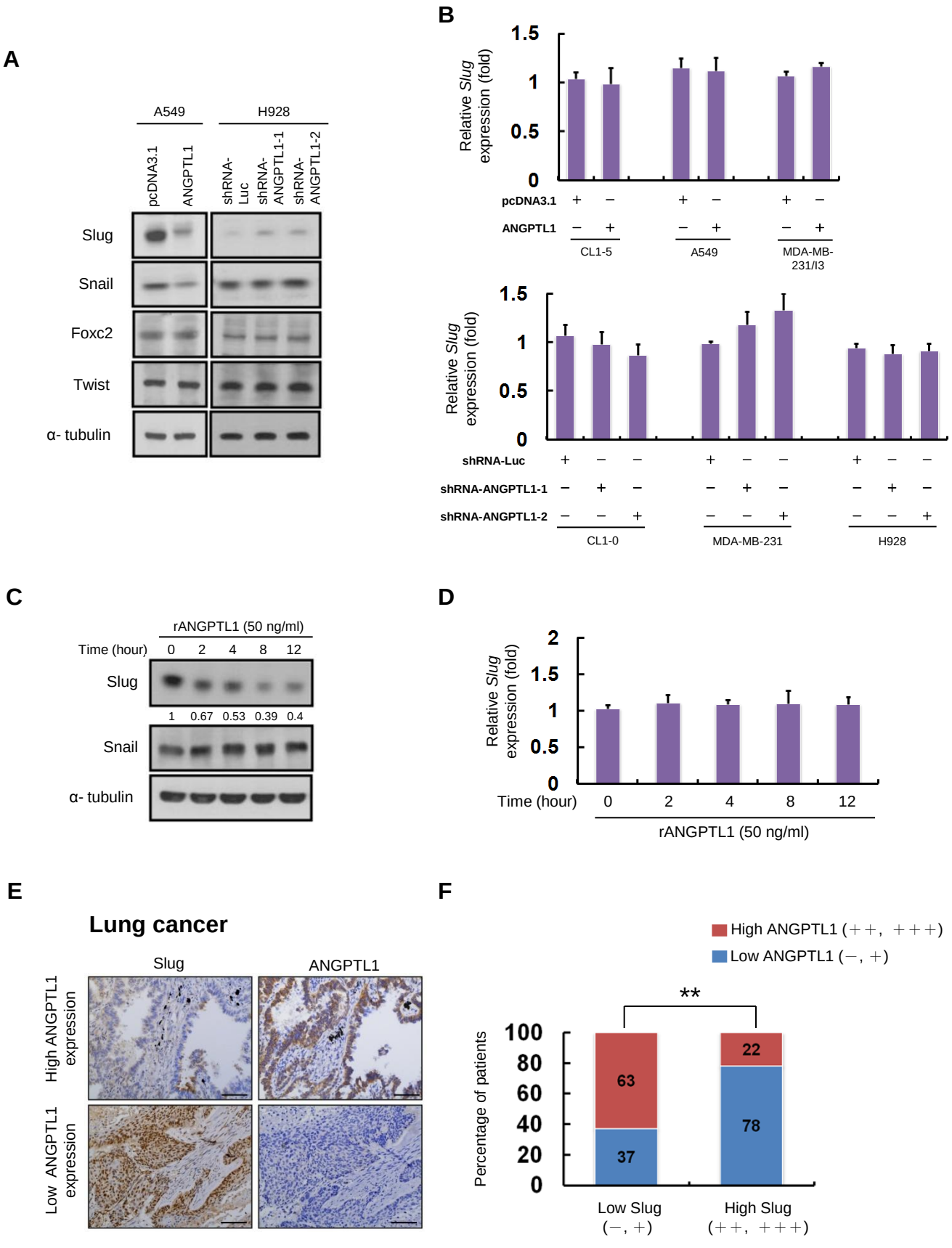

Supplementary Figure 6

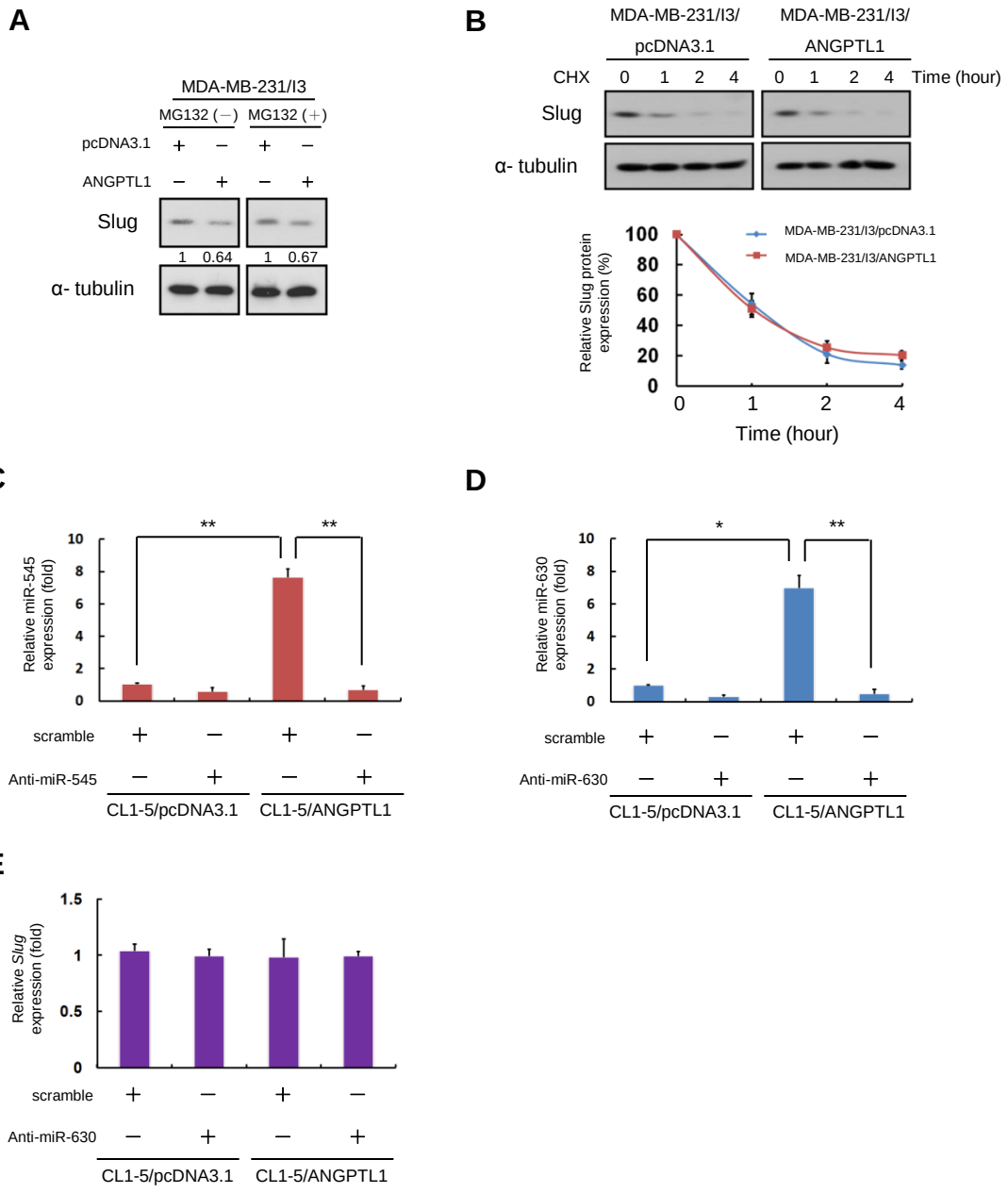

Supplementary Figure 7

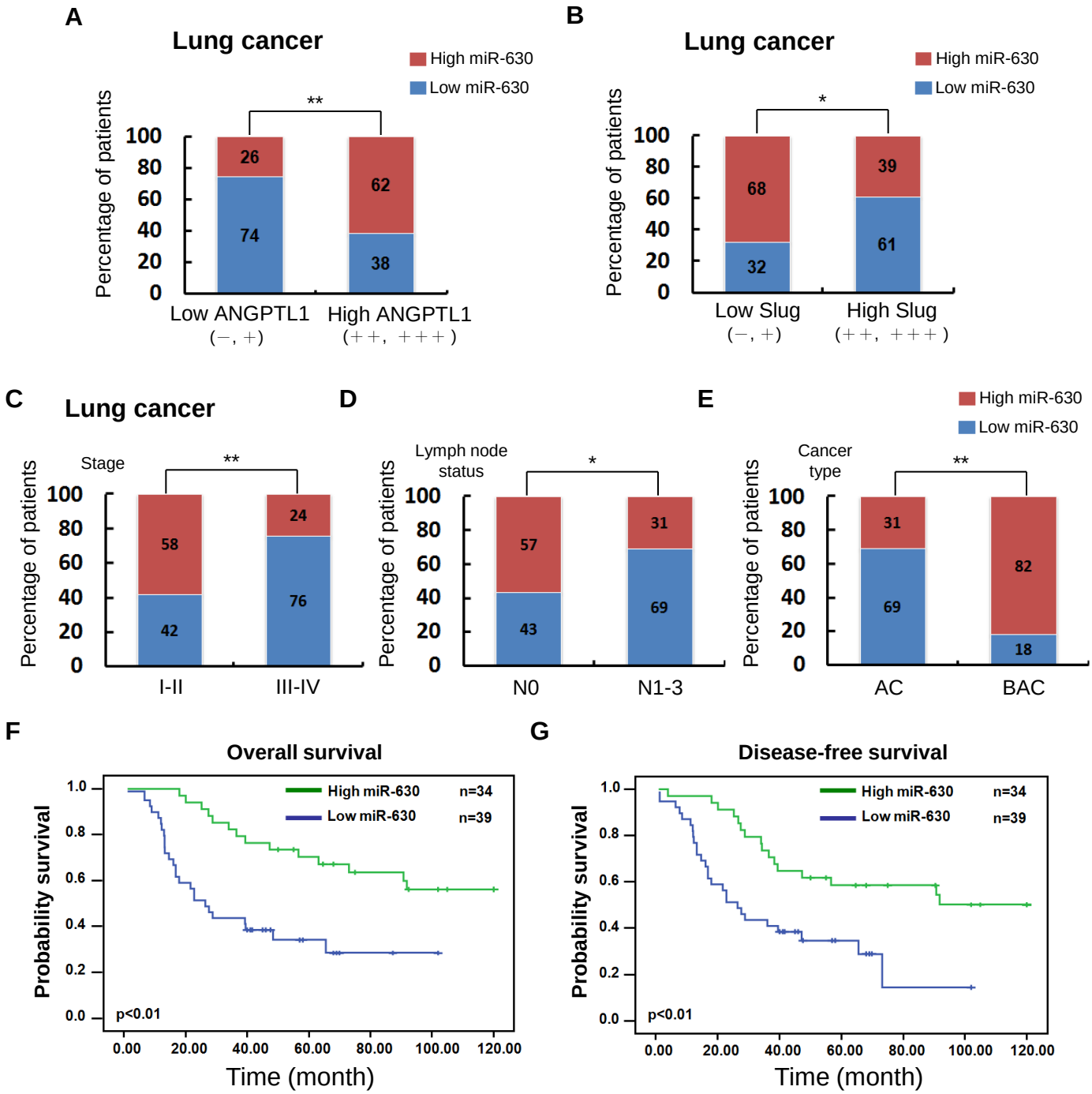

Supplementary Figure 8

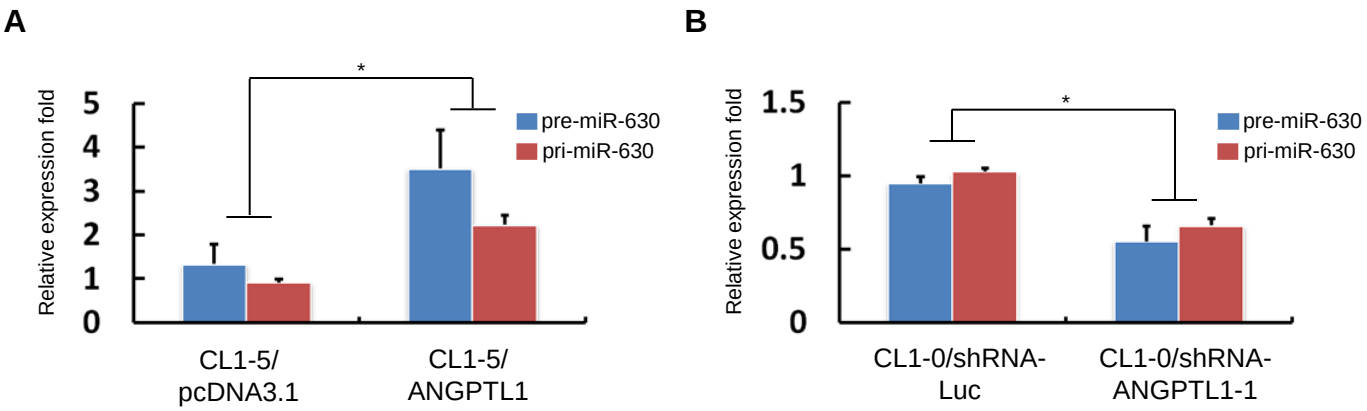

Supplementary Figure 9

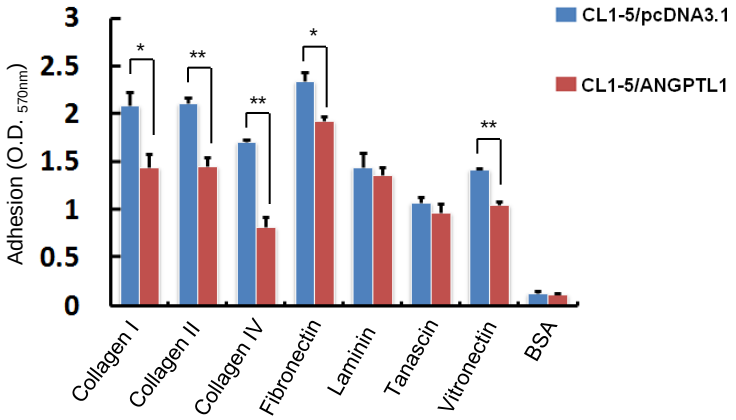

Supplementary Figure 10

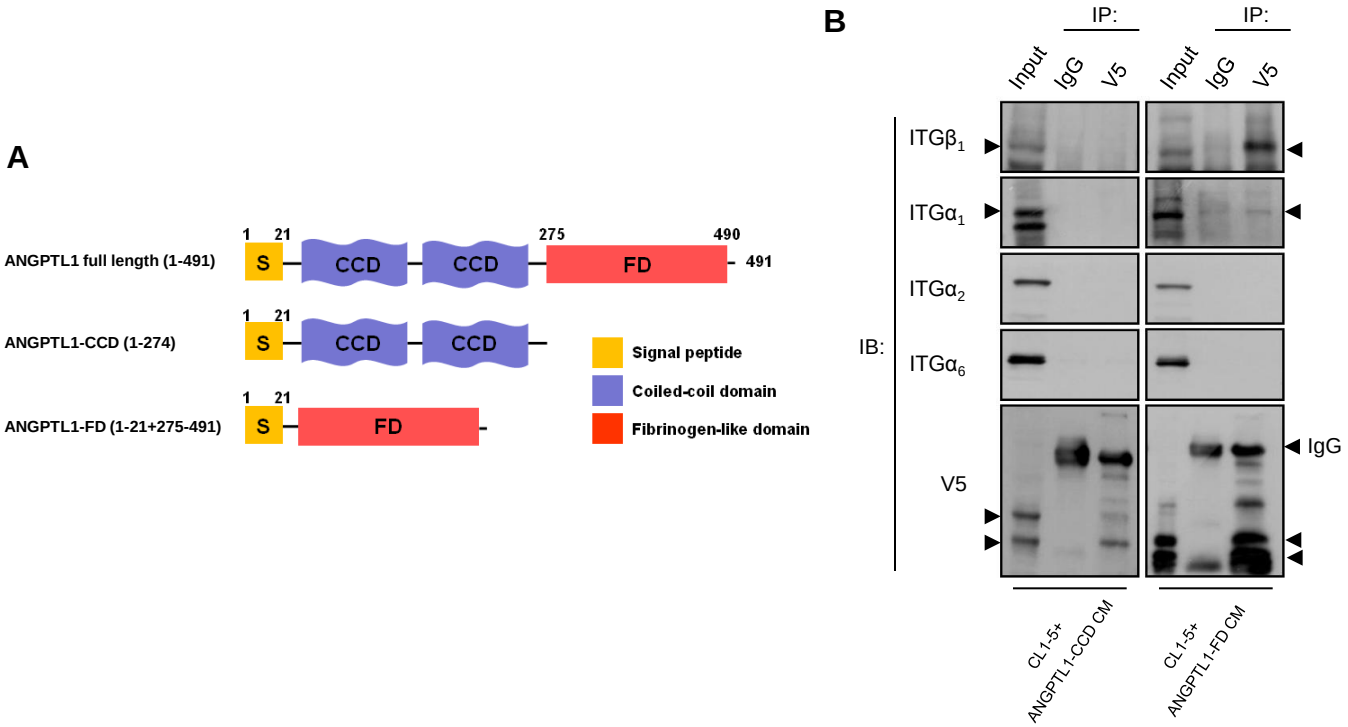

Supplementary Figure 11

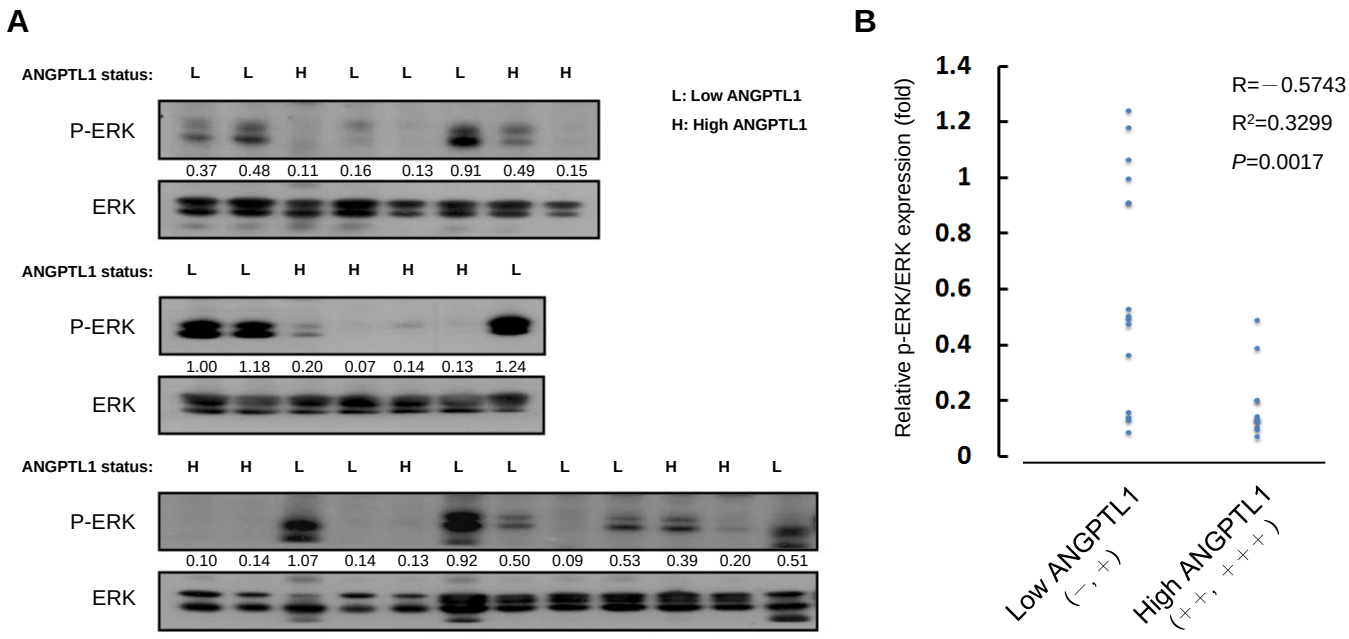

Supplementary Figure 12

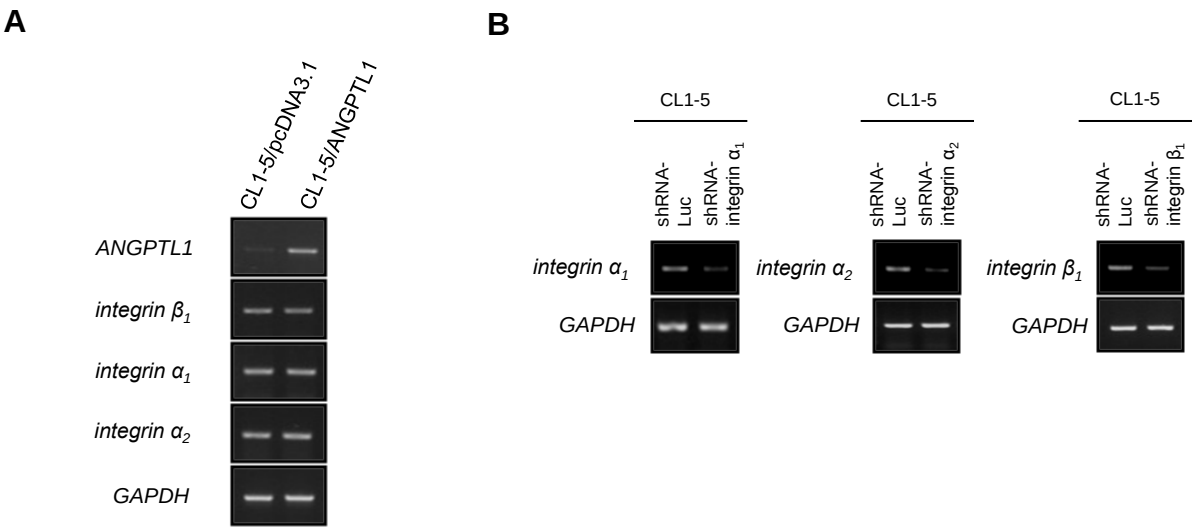

Supplementary Figure 13

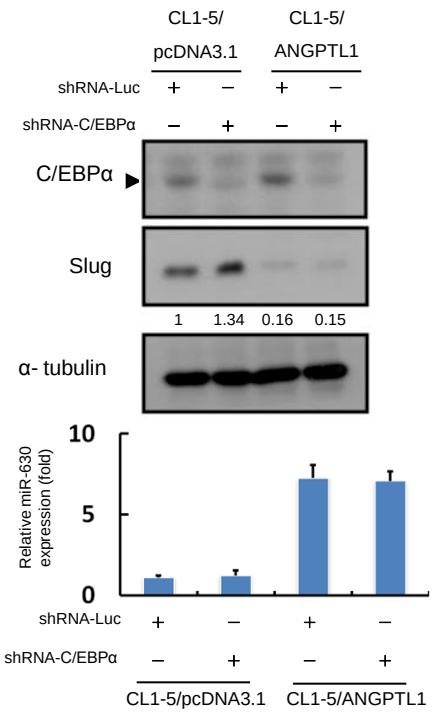

Supplementary Figure 14